Nuclear Engineering and Technology 54 (2022) 661–665

Contents lists available at ScienceDirect

Nuclear Engineering and Technology

journal homepage: www.elsevier.com/locate/net

Original article

Experimental investigation on the degradation of SiGe LNAs under different bias conditions induced by 3 MeV proton irradiation

Zhuoqi Li [a], Shuhuan Liu [a,*], Xiaotang Ren [b], Mathew Adefusika Adekoya [a], Jun Zhang [a], Shuangying Liu [a]

[a] Department of Nuclear Science and Technology, Xi'an Jiaotong University, Xi'an, 710049, China
[b] Proton Accelerator Laboratory, Peking University, Beijing, 100089, China

ARTICLE INFO

Article history:
Received 15 March 2021
Received in revised form
1 August 2021
Accepted 4 August 2021
Available online 6 August 2021

Keywords:
Proton irradiation damage
SiGe Low noise amplifier
Proton irradiation
S parameters
Noise figure

ABSTRACT

The 3 MeV proton irradiation effects on SiGe low noise amplifier (LNA) (NXP BGU7005) performance under different voltage supply VCC (0 V, 2.5 V) conditions were firstly experimental studied in this present work. The S parameters including S_{11}, S_{22}, S_{21}, 1 dB compression point and noise figure (NF) of the test samples under different bias voltage supply were measured and compared before and after 3 MeV proton irradiation. The total proton irradiation fluence was 1×10^{15} protons/cm^2. The maximum degradation quantities of the gain S_{21} and NF of the test samples under zero bias are measured respectively 1.6 dB and 1.2 dB. Compared with the samples under 2.5 V bias supply, the maximum degradation of S_{21} and NF are respectively 1.1 dB and 0.8 dB in the whole frequency band. It is noteworthy that the gain and NF of SiGe LNAs under zero-bias mode suffer enhanced degradation compared with those under normal bias supply. The key influence factors are discussed based on the correlation of the SiGe device and the LNA circuit. Different process of the ionization damage and displacement damage under zero-bias and 2.5 V bias voltage supply contributed to the degradation difference. The underlying physical mechanisms are analyzed and investigated.

1. Introduction

In commercial and military applications, there is a considerable trend to develop higher integrated electronic components and circuits on a single chip with multiple functions. The SiGe LNA integrating the high-speed SiGe HBTs and other functional circuits on a single chip with SiGe technology offers some unique advantages including high compact, low power consumption, super low temperature and noise performance, excellent total dose resistance, *etc* [1–5]. Therefore, LNA as one of the key components within the receiver chain of wireless system, it has the potential applications in harsh environment such as space and military special equipments. Despite SiGe HBT being confirmed to be robust to total ionizing dose (TID) effects, the inherent coupling between the physics of SiGe HBTs and the degradation response of the circuits under irradiation is still challenging [6]. Existing literatures reveal that SiGe LNA is still susceptible to TID effect. As shown in Refs. [7,8], the return loss, gain and noise figure of the zero-biased 0.13 μm SiGe LNA gradually degenerates with the increase of electron irradiation dose. In Refs. [9,10], 63.3 MeV proton irradiation experiments on the zero-biased 0.18 μm SiGe LNA were conducted. Slight degradations of the gain and noise figure are observed. However, the linearity performance of the SiGe LNA is not included in those studies. Besides, the fluence rate of 0.1–10 MeV proton is very high (~10^6 cm^{-2} s^{-1}) in the near-earth orbits [11,12] and little work has been devoted to the energy range. Although shielding materials can reduce the damage to circuits caused by low energy protons, more and more space exploration missions are now beginning to use non-shielded, anti-radiation circuits to reduce the electronic system's weight [13–19]. Further effort is required to understand the degradation performance of SiGe LNA induced by low energy proton.

Moreover, electronic devices are often under different biased mode in practical applications. To put it in practical terms, circuits operated in space applications are forward-biased when needed, while are usually floating or grounded at other times for power saving. Bias effects on performance degradation in SiGe HBTs irradiated by heavy ions and gamma rays are investigated in previous

* Corresponding author. Department of Nuclear Science and Technology, Xi'an Jiaotong University, No.25, Xianning West Road, Xi'an, Shaanxi, 710049, China.
E-mail addresses: li_zhuoqi@163.com (Z. Li), lsh_xjtuofficial@163.com (S. Liu).

https://doi.org/10.1016/j.net.2021.08.009
1738-5733/

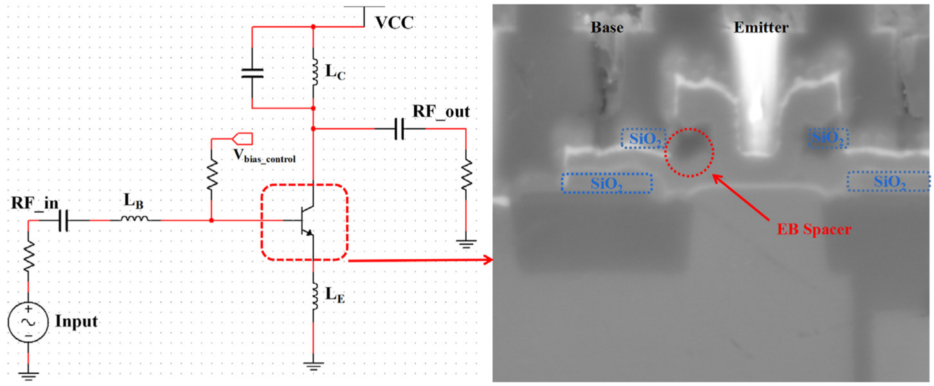

Fig. 1. Simplified circuit schematic and cross section of the SiGe HBT.

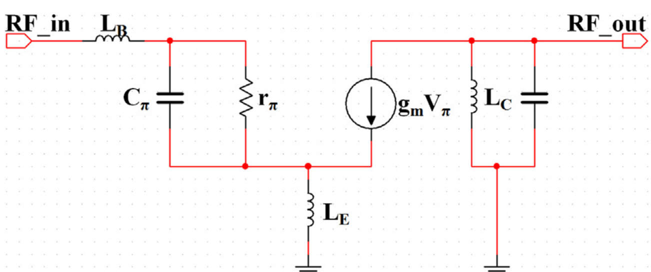

Fig. 2. Small signal model of the LNA with emitter degeneration.

studies [20–23]. However, the irradiation performance difference of SiGe LNA under normal bias and zero-bias mode is still unknown.

In this work, we aim to investigate the RF parameters response and degradation mechanisms of SiGe LNA under different bias conditions caused by low energy protons. First experimental results of 3 MeV proton irradiation on the 0.25 μm SiGe LNAs respectively under zero-bias and 2.5 V bias mode are presented. Section 2 begins by laying out the SiGe LNA topology and research methodology. In Section 3, the consolidated results are given and discussed. Conclusions are drawn in Section 4.

2. Experiment

2.1. The SiGe LNA topology

The test SiGe LNA (NXP BGU7005) samples used in this work are fabricated with 0.25 μm SiGe:C technology from the QUBiC4 process of NXP Semiconductors. Fig. 1 presents the simplified schematic as reported in Ref. [24] and the cross section of the SiGe HBT. The SiGe LNAs used for the Global Navigation Satellite System cover full L1 band frequency. The circuit topology consists of the adaptive biasing circuit and the common emitter transistor with the degeneration inductance.

Fig. 2 presents the simplified small signal model to provide insight into characteristics of the LNA. The LNA under test operate at 2.5 V and the measured S_{21} and noise figure is 18.4 dB and 0.73 dB at center frequency 1.6 GHz. For comparison of samples under different bias mode during irradiation, the S parameters and noise figures of LNA samples are measured from 1.4 GHz to 1.8 GHz before irradiation. The results show good consistency of samples. The input impedance Z_{in} can be given by Eq. (1), where L_E is the emitter degeneration inductance, C_π is the equivalent parasitic base emitter capacitance, g_m is the transconductance [25].

$$Z_{in} = \frac{g_m}{C_\pi} L_E + \frac{1}{sC_\pi} + s(L_B + L_E) \tag{1}$$

As reported in Refs. [25–27], the associate gain of the LNA mainly depends on the SiGe transistor transconductance g_m. The associate gain of the transistor can be expressed as Eq. (2), where $C_i = C_{BE} + C_{BC}$ and C_{BE}, C_{BC} is the SiGe HBT base-emitter and base-collector junction capacitance [27–29]. Considering the parasitic resistors in base and emitter (r_b, r_c), Eq. (3) presents the noise factor of the LNA with inductor degeneration [27,30,31].

$$G_A \cong \frac{1}{\omega^2 r_b C_{BC} C_i} \sqrt{\left(\frac{g_m r_b + 0.5}{2} \frac{g_m{}^2}{\beta} \right) + \frac{(\omega C_i)^2}{2} g_m r_b} \tag{2}$$

$$NF = 1 + \frac{r_b + r_c}{Z_0} + \frac{g_m}{2} Z_0 \left(\frac{f_T}{f} \right)^2 \tag{3}$$

It is noted that the performance of the SiGe LNA is influenced by several factors included base and emitter resistance, junction capacitance, transistor transconductance and transistor DC gain β.

For comparison of samples under different bias mode during irradiation, the S parameters and noise figures of LNA samples are measured from 1.4 GHz to 1.8 GHz before irradiation. The gain S_{21} and noise figure of the LNAs under normal 2.5 V bias supply are measured respectively 18.4 dB and 0.73 dB at center frequency 1.6 GHz. The results show good consistency of the test samples.

2.2. Irradiation and measurement methods

Samples were exposed to 3 MeV at room temperature in the Proton Accelerator Laboratory located at the Peking University. The whole evaluation boards are attached to an aluminum alloy holder in the irradiation vacuum chamber and the package lids of samples are removed to ensure the accuracy of proton irradiation. The proton beam area can be located by the fluorescent bars observed in the control room. The Faraday cup is used to measure the beam intensity, and the beam current integrator controls the flux and irradiation time. Two bias conditions were applied during exposure: (1) zero-bias mode (VCC = 0 V). (2) normal 2.5 V bias mode (VCC = 2.5 V). After 1×10^{15} protons/cm^2 irradiation, LNAs were taken out and measured immediately. S parameters were measured by Tekronix RSA306 vector network analyzer, and noise figure was measured by Agilent N8975A noise figure analyzer. Calibration was carried out before each measurement to make sure the data accuracy.

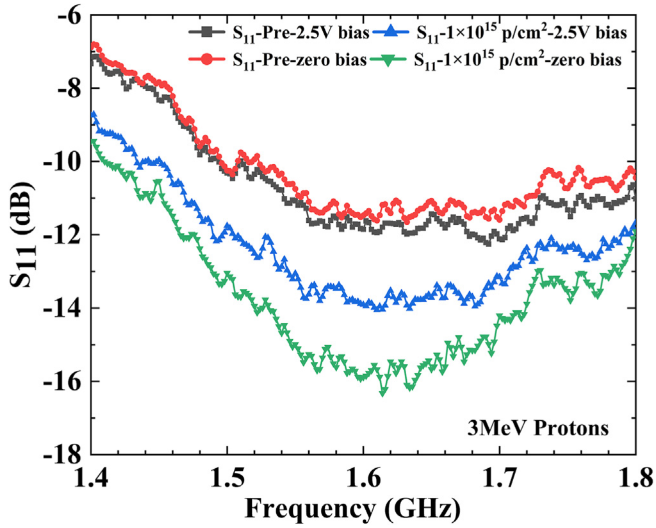

Fig. 3. Pre- and post-radiation S_{11} for 2.5 V bias and zero-bias mode.

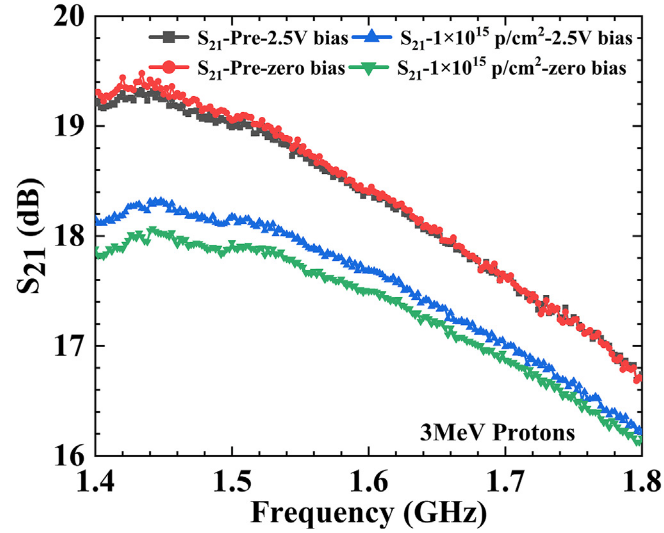

Fig. 5. Pre- and post-radiation S_{21} for 2.5 V bias and zero-bias mode.

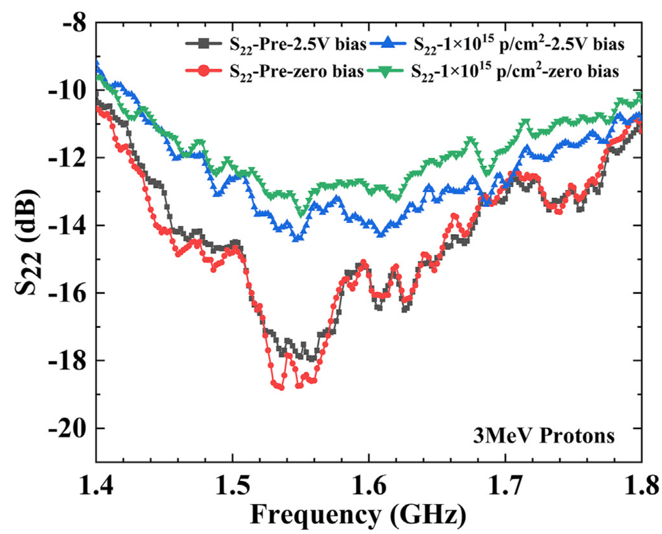

Fig. 4. Pre- and post-radiation S_{22} for 2.5 V bias and zero-bias mode.

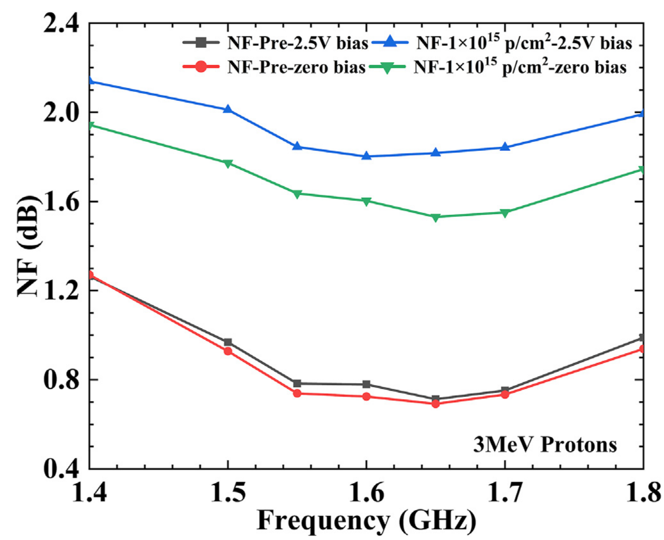

Fig. 6. NF as the function of frequency for 2.5 V-bias and zero-bias mode.

3. Results and discussion

Fig. 3 and Fig. 4 present an overview of the input return loss S_{11} and output return loss S_{22}, respectively. Both the S_{11} decrease and S_{22} increase after irradiation under different bias mode. As compared with the return loss under 2.5 V bias mode, what stands out is the changes in return loss are much larger under zero-bias mode. Similarly, degradation of gain S_{21} and noise figure NF are more severe under zero-bias mode as shown in Fig. 5 and Fig. 6.

From Eq. (1), it can be found that the S_{11} is mainly correlated with the base-emitter capacitance C_{BE} and the transconductance g_m. As reported in Ref. [26], the traps or defects in EB spacer region marked in Fig. 1 and incomplete bonding at the surfaces of the dielectric induced by ionization damage results in an increase of the dielectric constant. This, in turn, increased the EB junction capacitance. Besides, proton irradiation degrades the diffusion length and mobility of carriers in the transistor, which in turn leads to a lifetime decrease of minority carriers, and then causes a significant decrease in g_m as the irradiation fluence increases [32]. This is also confirmed by Refs. [26,33]. Thus, the parameter S_{11} changing trends of the experimental samples under different bias conditions after proton irradiation may be caused by the synthesized influence of the base-emitter C_{BE} and transconductance g_m. As for the increased S_{22} shown in Fig. 4, it indicated the output loss were worse after irradiation which may due to the change of the output impedance. From Eq. (2), it noted that the increased r_b and C_{BE} and the reduction of g_m after proton irradiation dominated the degradation of S_{21}. The increased base resistance (r_b) can be attributed to two factors. On one hand, the carrier removal and coulomb scattering of the carrier result by proton-induced traps would lead to the increase of the base resistance [10]. Besides, the deep-shallow defect energy level introduced by displacement effect will decrease the quantity of carriers and bring about the deactivation of dopant which may also responsible for the increase of base resistant [33,34]. These factors lead to the degradation as well as the linearity of the LNA, evidenced by the measured input 1 dB compression (P1dB) as shown in Fig. 7.

From Eq(4), it can be seen that the degradation of NF also come from the increase of emitter and base thermal noise due to the increased base and emitter resistance, as well as the decrease of g_m

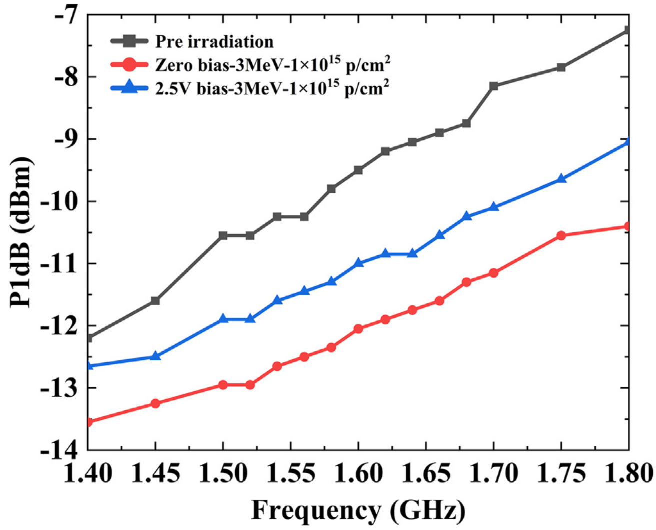

Fig. 7. Pre- and post-radiation input P1dB under zero-bias and 2.5 V bias mode.

as mentioned above. Moreover, in Ref. [33], it noted that NF_{min} obtained from the input noise matching is changed due to the change of the optimum reflection coefficient after proton irradiation. The measured input return loss (Fig. 3) confirmed the change of the input impedance matching.

In order to clearly compare the degradation difference under different bias conditions, Table 1 presents the measured RF parameters at the central frequency 1.6 GHz under zero-bias and 2.5 V bias mode. The S_{21} and NF of the SiGe LNA under zero-bias mode show larger degradation compared with 2.5 V bias mode. It indicated that after the same dose proton irradiation, the zero-biased SiGe LNA suffers enhanced degradation compared with that at normal bias supply. The similar results are also observed in SiGe transistors as reported in Refs. [20,23].

Table 1
Result comparison of proton irradiation on SiGe LNA.

Reference	[9]	[10]	this work	this work
Proton Energy	63.3 MeV	63.3 MeV	3 MeV	3 MeV
Bias Mode	zero-bias	zero-bias	zero-bias	2.5 V bias
f_0 (GHz)	12	62	1.6	1.6
Total Dose	2 Mrad	0.134 Mrad	1×10^{15} p/cm^2	
Pre-S_{11} (dB)	–	–	−11.6	−11.8
Post-S_{11} (dB)	–	–	−15.9	−14.1
Pre-$S_{21(max)}$ (dB)	17.5	14.2	18.4	18.4
Post-$S_{21(max)}$ (dB)	17.3	13.6	17.1	17.7
Pre-NF (dB)	5.85	3	0.73	0.78
Post-NF (dB)	5.63	3.5	1.8	1.6
Pre-input P1dB (dBm)	–	–	−7.4	−7.4
Post-input P1dB (dBm)	–	–	−12.05	−11

On one hand, the performance difference is attributed to the effects of the fringe electric field in SiO_2 layer and applied electric field of the SiGe HBT as shown in Fig. 8. Most of the electron-hole pairs induced by proton irradiation will recombine in a very short time, then the remaining electrons in SiO_2 layers of p-n junction will immediately drift out of the oxide layer, while the holes will be captured by the traps near the surface and become the net positive oxide trapped charge [35]. In addition, the hydrogen ions released by the holes will diffuse to the *Si*—SiO_2 interface and then react with *Si*—H passivated bond to form the interface defects [36]. Both the positive oxide trapped charge and the interface defects would result in the degradation of the SiGe HBT, and subsequently influence the RF performance of the SiGe LNA.

Compared to the zero-bias state, the applied normal voltage bias weakened the fringe electric field results in more recombination of electron-hole pairs caused by proton irradiation and less remaining holes in SiO_2 layer, hence the net positive oxide trapped holes and the interface defects are decreased. This in turn reduced the ionization damage for 2.5 V bias LNA. Another factor may attribute to the injection annealing of displacement caused by high dose proton irradiation [21]. The electron injection under 2.5 V bias state result in the increase of vacancy mobility and then reducing the concentration of displacement damage caused the less performance degradation. Table 1 also compares this work with other researches on SiGe LNA irradiated by proton based on limited open source data. The result difference between this work and Refs. [9,10] may attribute different proton energy and SiGe circuit topology. Previous studies [20,23] display that bipolar transistors are more severely damaged by low-energy proton irradiation than high-energy proton irradiation. It may be one possible reason for that the degradation of the LNAs under 3 MeV proton irradiation is much more than under 63.3 MeV proton irradiation. However, further investigations are needed for radiation response of SiGe LNA fabricated with different technique.

4. Conclusion

The degradation response of 3 MeV proton irradiation on 0.25 μm SiGe LNAs (NXP BGU7005) under zero-bias (VCC = 0 V) and normal bias (VCC = 2.5 V) modes respectively are experimental investigated for the first time in the present work. The typical parameters (S parameter, NF and P1dB) of the test samples under different bias voltage supply are measured, compared and analyzed before and after 1×10^{15} protons/cm^2 irradiation. The 3 MeV proton irradiation can introduce both the ionizing total dose and displacement damage in the test samples according to physical mechanisms of the proton interaction with materials.

The input loss S_{11} decreased and output loss S_{22} increased after 3 MeV proton irradiation. Clear reduction of forward gain (S_{21}) and increasing of noise figure (NF) of the test samples under different bias modes are observed in the whole frequency band after irradiation. It is found that the RF performance of the SiGe LNA samples

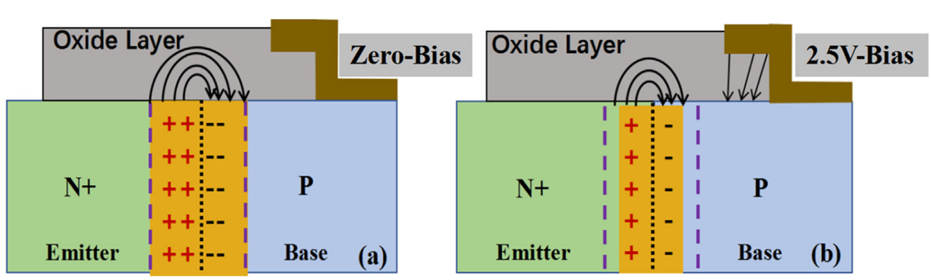

Fig. 8. The electric field distributions in the EB junction under zero-bias and 2.5 V bias conditions.

degraded more seriously at zero bias state than those at normal bias. The mechanisms may mainly be related with the increasing junction resistance (r_b, r_c), decreasing transconductance g_m and interface state of the embedded SiGe HBTs in the sample chip after extreme proton radiation.

Declaration of competing interest

The authors declare that they have no known competing financial interests or personal relationships that could have appeared to influence the work reported in this paper.

Acknowledgements

This work was supported by the National Natural Science Foundation of China (NSFC) under grants NO. 12075180 and 11575139. The authors would like to thank the Peking University Proton Accelerator Laboratory team.

References

[1] N. Logan, J.M. Noras, Advantages of bipolar SiGe over silicon CMOS for a 2.1 GHz LNA, in: 2009 9th Int. Conf. Telecommun. Mod. Satell. Cable Broadcast. Serv., 2009, pp. 29–31, https://doi.org/10.1109/TELSKS.2009.5339497.
[2] W. Lambrechts, S. Sinha, A review on Si, SiGe, GaN, SiC, InP and GaAs as enabling technologies in EW and space, in: SiGe-Based Re-eng. Electron. Warf. Subsystems, Springer International Publishing, Cham, 2017, pp. 301–329, https://doi.org/10.1007/978-3-319-47403-8_10.
[3] J.D. Cressler, On the potential of SiGe HBTs for extreme environment electronics, Proc. IEEE 93 (2005) 1559–1582, https://doi.org/10.1109/JPROC.2005.852225.
[4] J.D. Cressler, Silicon-germanium as an enabling technology for extreme environment electronics, IEEE Trans. Device Mater. Reliab. 10 (2010) 437–448, https://doi.org/10.1109/TDMR.2010.2050691.
[5] J.D. Cressler, Radiation effects in SiGe technology, IEEE Trans. Nucl. Sci. 60 (2013) 1992–2014, https://doi.org/10.1109/TNS.2013.2248167.
[6] J.D. Cressler, Device-to-circuit interactions in SiGe technology: challenges and opportunities, in: 2014 IEEE BipolarBiCMOS Circuits Technol. Meet. BCTM, 2014, pp. 45–55, https://doi.org/10.1109/BCTM.2014.6981283.
[7] A.S. Youssouf, M.H. Habaebi, S.N. Ibrahim, N.F. Hasbullah, Gain investigation for commercial GaAs and SiGe HBT LNA's under electron irradiation, in: 2016 IEEE Stud. Conf. Res. Dev. SCOReD, 2016, pp. 1–5, https://doi.org/10.1109/SCORED.2016.7810094.
[8] F.S. Minko, T. Stander, Effect of TID electronradiation on SiGe BiCMOS LNAs at V-band, Microelectron. Reliab. 112 (2020) 113750, https://doi.org/10.1016/j.microrel.2020.113750.
[9] D.C. Howard, P.K. Saha, S. Shankar, R.M. Diestelhorst, T.D. England, N.E. Lourenco, E. Kenyon, J.D. Cressler, An 8–16 GHz SiGe low noise amplifier with performance tuning capability for mitigation of radiation-induced performance loss, IEEE Trans. Nucl. Sci. 59 (2012) 2837–2846, https://doi.org/10.1109/TNS.2012.2224132.
[10] Wei-Min Lance Kuo, Yuan Lu, B.A. Floyd, B.M. Haugerud, A.K. Sutton, R. Krithivasan, J.D. Cressler, B.P. Gaucher, P.W. Marshall, R.A. Reed, G. Freeman, Proton radiation response of monolithic Millimeter-wave transceiver building blocks implemented in 200 GHz SiGe technology, IEEE Trans. Nucl. Sci. 51 (2004) 3781–3787, https://doi.org/10.1109/TNS.2004.839215.
[11] N.A. Dodds, M.J. Martinez, P.E. Dodd, M.R. Shaneyfelt, F.W. Sexton, J.D. Black, D.S. Lee, S.E. Swanson, B.L. Bhuva, K.M. Warren, R.A. Reed, J. Trippe, B.D. Sierawski, R.A. Weller, N. Mahatme, N.J. Gaspard, T. Assis, R. Austin, S.L. Weeden-Wright, L.W. Massengill, G. Swift, M. Wirthlin, M. Cannon, R. Liu, L. Chen, A.T. Kelly, P.W. Marshall, M. Trinczek, E.W. Blackmore, S. Wen, R. Wong, B. Narasimham, J.A. Pellish, H. Puchner, The contribution of low-energy protons to the total on-orbit SEU rate, IEEE Trans. Nucl. Sci. 62 (2015) 2440–2451, https://doi.org/10.1109/TNS.2015.2486763.
[12] Q. Yu, L. Luo, M. Tang, Y. Sun, Z. Wei, Z. Li, M. Zhu, Experimental study of 0.18μm and 65nm SRAM SEUs induced by heavy ions, high energy protons and low energy protons on orbits, in: 2015 15th Eur. Conf. Radiat. Its Eff. Compon. Syst. RADECS, 2015, pp. 1–5, https://doi.org/10.1109/RADECS.2015.7365612.
[13] O. Kegege, M. Barlow, A. Mantooth, R. Ulrich, Mission optimization and tradeoffs of using SiGe based electronics for a cryogenic environment rover mission, in: 2010 IEEE Aerosp. Conf., 2010, pp. 1–6, https://doi.org/10.1109/AERO.2010.5446757.
[14] W. Lambrechts, S. Sinha, SiGe for radiation hardening: spearheading electronic warfare in space, in: SiGe-Based Re-eng. Electron. Warf. Subsystems, Springer International Publishing, Cham, 2017, pp. 201–233, https://doi.org/10.1007/978-3-319-47403-8_7.
[15] K. Clark, G. Tan-Wang, J. Boldt, R. Greeley, I. Jun, R. Lock, J. Ludwinski, R. Pappalardo, T.V. Houten, T. Yan, Return to europa: overview of the jupiter europa orbiter mission, in: 2009 IEEE Aerosp. Conf., 2009, pp. 1–20, https://doi.org/10.1109/AERO.2009.4839315.
[16] I. Song, Design of SiGe BICMOS RF Building Blocks for Extreme-Environment Applications, Georgia Institute of Technology, 2016.
[17] P.C. Adell, J. Yager, Z. Pannell, J. Shelton, M.M. Mojarradi, B. Blalock, G. Allen, R. Some, Radiation hardening of an SiGe BiCMOS wilkinson ADC for distributed motor controller application, IEEE Trans. Nucl. Sci. 61 (2014) 1236–1242, https://doi.org/10.1109/TNS.2014.2323975.
[18] T. England, C. Chatterjee, N. Lourenco, S. Finn, L. Najafizadeh, S. Phillips, E. Kenyon, R. Diestelhorst, J. Cressler, Cold-capable, radiation-hardened SiGe BiCMOS wireline transceivers, IEEE Aero. Electron. Syst. Mag. 29 (2014) 32–41, https://doi.org/10.1109/MAES.2014.6805364.
[19] Z.E. Fleetwood, E.W. Kenyon, N.E. Lourenco, S. Jain, E.X. Zhang, T.D. England, J.D. Cressler, R.D. Schrimpf, D.M. Fleetwood, Advanced SiGe BiCMOS technology for multi-mrad electronic systems, IEEE Trans. Device Mater. Reliab. 14 (2014) 844–848, https://doi.org/10.1109/TDMR.2014.2331980.
[20] Y. Sun, Z. Liu, J. Fu, X. Li, Y. Shi, Investigation of total dose effects in SiGe HBTs under different exposure conditions, Radiat. Phys. Chem. 151 (2018) 84–89, https://doi.org/10.1016/j.radphyschem.2018.05.019.
[21] Y. Sun, J. Fu, J. Xu, Y. Wang, W. Zhou, W. Zhang, J. Cui, G. Li, Z. Liu, Impact of bias conditions on performance degradation in SiGe HBTs irradiated by 10MeV Br ion, Microelectron. Reliab. 54 (2014) 2728–2734, https://doi.org/10.1016/j.microrel.2014.08.010.
[22] J. Zhang, Q. Guo, H.-X. Guo, W. Lu, C. He, X. Wang, P. Li, L. Wen, Investigation of enhanced low dose rate sensitivity in SiGe HBTs by 60Co γ irradiation under different biases, Microelectron. Reliab. 84 (2018) 105–111, https://doi.org/10.1016/j.microrel.2018.03.007.
[23] S. Zhang, J.D. Cressler, G. Niu, C.J. Marshall, P.W. Marshall, H.S. Kim, R.A. Reed, M.J. Palmer, A.J. Joseph, D.L. Harame, The effects of operating bias conditions on the proton tolerance of SiGe HBTs, Solid State Electron. 47 (2003) 1729–1734, https://doi.org/10.1016/S0038-1101(03)00131-X.
[24] A.B. Smolders, H. Gul, E. v d Heijden, P. Gamand, M. Geurts, BiCMOS high-performance ICs: from DC to mm-wave, in: 2009 IEEE BipolarBiCMOS Circuits Technol. Meet., 2009, pp. 115–122, https://doi.org/10.1109/BIPOL.2009.5314130.
[25] D.C. Howard, X. Li, J.D. Cressler, A low power 1.8–2.6 dB noise figure, SiGe HBT wideband LNA for multiband wireless applications, in: 2009 IEEE BipolarBiCMOS Circuits Technol. Meet., 2009, pp. 55–58, https://doi.org/10.1109/BIPOL.2009.5314152.
[26] B. Habeenzu, TID Induced Small Signal Model Variation in CMOS and SiGe BiCMOS, University of Pretoria, 2019.
[27] J. Cressler, in: Silicon-Germanium Heterojunction Bipolar Transistor, 2001, pp. 69–84, https://doi.org/10.1007/978-1-4757-3318-1_4.
[28] J. Alvin, S. Ananth, P. Shrinivas, Z. Mike, J. Vibhor, L. Chaojiang, A. James, High-resistivity SiGe BiCMOS for switch+LNA integration for WiFi front-end IC applications, in: 2016 13th IEEE Int. Conf. Solid-State Integr. Circuit Technol. ICSICT, 2016, pp. 57–60, https://doi.org/10.1109/ICSICT.2016.7998838.
[29] Guofu Niu, J.D. Cressler, Shiming Zhang, A. Joseph, D. Harame, Noise-gain tradeoff in RF SiGe HBTs, in: 2001 Top. Meet. Silicon Monolith. Integr. Circuits RF Syst. Dig. Pap. IEEE Cat No01EX496, 2001, pp. 187–191, https://doi.org/10.1109/SMIC.2001.942363.
[30] H. Xie, Z. Lu, W. Zhang, P. Shen, C. Ding, Y. You, B. Sun, A dual-band SiGe HBT low noise amplifier, in: 2010 10th IEEE Int. Conf. Solid-State Integr. Circuit Technol., 2010, pp. 668–670, https://doi.org/10.1109/ICSICT.2010.5667287.
[31] Z. Yang, Niehai, W. Han, A high-linearity S-band SiGe HBT low-noise amplifier design, in: 2013 Int. Workshop Microw. Millim. Wave Circuits Syst. Technol., 2013, pp. 308–311, https://doi.org/10.1109/MMWCST.2013.6814639.
[32] A.P.G. Prakash, T.M. Pradeep, V.N. Hegde, N. Pushpa, P.K. Bajpai, S.P. Patel, T. Trivedi, K.G. Bhushan, Comparison of effect of 5 MeV proton and Co-60 gamma irradiation on silicon NPN rf power transistors and N–channel depletion MOSFETs, Radiat. Eff. Defect Solid 172 (2017) 952–963, https://doi.org/10.1080/10420150.2017.1421189.
[33] Shiming Zhang, Guofu Niu, J.D. Cressler, S.D. Clark, D.C. Ahlgren, The effects of proton irradiation on the RF performance of SiGe HBTs, IEEE Trans. Nucl. Sci. 46 (1999) 1716–1721, https://doi.org/10.1109/23.819144.
[34] Yuan Lu, J.D. Cressler, R. Krithivasan, Ying Li, R.A. Reed, P.W. Marshall, C. Polar, G. Freeman, D. Ahlgren, Proton tolerance of third-generation, 0.12/spl mu/m 185 GHz SiGe HBTs, IEEE Trans. Nucl. Sci. 50 (2003) 1811–1815, https://doi.org/10.1109/TNS.2003.820737.
[35] S.T. Pantelides, Z.-Y. Lu, C. Nicklaw, T. Bakos, S.N. Rashkeev, D.M. Fleetwood, R.D. Schrimpf, The E′ center and oxygen vacancies in SiO2, J. Non-Cryst. Solids 354 (2008) 217–223, https://doi.org/10.1016/j.jnoncrysol.2007.08.080.
[36] D.M. Fleetwood, S.T. Pantelides, S.N. Rashkeev, R.D. Schrimpf, Defect generation by hydrogen at the Si-SiO2 interface, Phys. Rev. Lett. 87 (2001) 165506.